# EFFECT OF SURFACE BRAIDED ANGLE ON VIBRATION MODAL OF A NOVEL THREE-DIMENSION AND FOUR-DIRECTION BRAIDED COMPOSITE T-BEAM

Xiaoyuan Pei [1, 2, 3], Huan Wang [1], Li Chen [1], Jialu Li [1, 2, *], Youhong Tang [3, *]

[1] Composites Research Institute and Education Ministry Key Laboratory of Advanced Textile Composite Materials, Tianjin Polytechnic University, Tianjin 300160, China.
[2] School of Material Science and Engineering and State Key Laboratory of Separation Membranes and Membrane Processes, Tianjin Polytechnic University, Tianjin 300387, China.
[3] Institute of NanoScale Science & Technology, Flinders University, South Australia 5042, Australia.

[*]Corresponding authors: Tel.: +86 22 24528052, E-mail address: lijialu@tjpu.edu.cn (J Li) and Tel.: +61 8 82012128, E-mail: youhong.tang@flinders.edu.au (Y Tang).

**Keywords:** *Polymer-matrix composite (PMCs), Vibration, Finite element analysis (FEA), Braiding*

## ABSTRACT

Carbon fibre reinforced polymer (CFRP) composites are increasingly used in the aerospace field to reduce the weight and improve the stability of structures. In most conditions, micro-cracks presented in these structures propagate rapidly due to fatigue caused by vibrations, resulting in premature failure. In high-precision space missions, the structural design and dynamic performance of CFRP composites are integral to the performance of the spacecraft. This study focuses on the influence of a novel three-dimension (3 Dim) and four-direction (4 Dir) braided composite T-beam structural design on vibration properties. The effects of surface braided angles and geometry on the modal properties of the T-beam are investigated by means of modal experiments and finite element analysis. The results show that the structural design of the T-beam can meet various requirements of dynamic performance.

## 1 INTRODUCTION

The T-beam is a component used extensively in engineering structures. In the field of aeronautics, use of metal T-beams is limited because of their low specific strength and stiffness. Compared with metal T-beams, composite T-beams have lower density, higher specific strength and modulus, and thus are often used in aircraft fuselages, wings, and joints to carry load and resist surface deformation. The mechanical properties of composite T-beams have been studied extensively. Compared with the traditional laminated composite, the potential applications of three-dimensional (3 Dim) braided composites are very broad, by virtue of their integrated non-delaminating structure, high specific strength, high specific stiffness, and excellent ablation resistance [1-2]. In particular, the near-net shape forming capacity to manufacture its final shape without machining can avoid damaging the reinforced fibres [3-4]. Thus, a major contribution to weight reduction and desirable mechanical properties is possible with the replacement of metal T-beams with composite ones, such as titanium alloys and high-temperature alloys.

Composites have extensive applications because their mechanical properties can be enhanced or tuned to meet the extraordinary requirements of harsh service conditions by incorporating the advantages of their individual components and by their precise manufacturing technology. Most service conditions for such composites involve dynamic loads. For that reason, the effects of composites' dynamic behaviour have aroused increasing interest. For example, a general analytical model applicable to the vibration analysis of thin-walled composite I-beams with arbitrary lay-ups was developed by Lee et al. [5]. The effects of fibre orientation, location of applied load, and types of load on the natural frequencies and load-frequency interaction curves as well as vibration mode shapes have been parametrically studied. In 2009, Minghini et al. [6] analysed the vibration analysis of the thin-walled beams and framework of pultruded FRP laminated composites. The vibration frequencies and mode shapes of pultruded glass FRP portal frames were extensively evaluated as a function of the applied loads, and sudden exchanges of fundamental modes were noted. Tran et al. [7] computed

---

stress intensity factors under dynamic loading conditions at low frequency with an extended finite element method (FEM). Yesilyurt et al. [8] studied the application of vibration analysis in the determination of elastic constants and modal damping ratios of a unidirectional composite beam.

Some researchers have gone so far as to predict damping characteristics. For example, Kyriazoglou et al. [9] used a mixed method to predict the damping characteristic of a vibration laminated composite. They showed that with that methodology, damping data could be extracted for cases in which the application of continuum mechanics analytical solutions could not provide reliable information. Jin et al. [10] studied a unified method for the vibration and damping analysis of constrained layer damping cylindrical shells with arbitrary boundary conditions. In their research, an accurate solution was developed for the vibration and damping characteristics of a three-layered passive constrained layer damping cylindrical shell with general elastically restrained boundaries. Our group has carried out preliminary research on the dynamic behaviour of braided composites. For example, Li et al. [11] studied the vibration damping properties of a 3 Dim braided composite using an experimental method of the free vibration damping of cantilever beams, and analysed the influence of braiding angle, fibre volume fraction ($V_f$), and braiding structure on a 3 Dim braided composite. Gao et al. [12] conducted a vibration modal experiment for the cantilever of 3 Dim and five-directional (5 Dir) braided composites. Their experimental results showed that with an increase in fibre orientation angle, the natural frequency of the composite decreased and the loss factor increased. We also used discrete beam modals to explore the effect rule of microstructure properties on the dynamic parameters of the composite [13].

Micro structure and geometry of 3D braided composite T beams are the key factors influencing the vibration characteristics. The braided angle is an important micro structural parameter when determining the properties of braided composites. The size of the braided angle directly affects the direction of the fibre bundles in 3D braided composites and affects the properties of the materials [14]. The braided angle is affected by microscale parameters, and those parameters together determine the braided angle value. To obtain the optimal solution for various performance requirements, the design and optimization of the material need to be known to reflect the performance index in the change of each parameter [15]. Under the cantilever beam boundary condition, finite element simulation was used to investigate the influence of structural parameters (micro structure and geometry) on vibration characteristics of T beam. The effects of surface braided angle on the natural frequency and mode shape of the T-beam were investigated. The influence of geometry on the natural frequency of T beam was calculated when the micro structure parameters was constant. The relationship between the natural frequency and the geometry of the reinforcing plate and web plate is analysed. To validate the simulation model, the corresponding experiments were performed. According to the relationship between the braided angle and the structure of the braided composite preform, a CFRP T-beam specimen was designed [16]. Using the same boundary conditions and material properties, the influences of the microstructure and the length of the free end on the modal properties of T beam were analysed. The experimental vibration modal analysis and simulation were compared to obtain consolidated results. Through the design of micro structure parameters and the selection of geometry, the modal parameters of 3D braided composite T beam can be designed. It provides a strong basis for the design and application of a T beam in a vibration environment.

## 2 EXPERIMENTS AND CHARCTERSATIONS

### 2.1 Materials and preparation

Our previous report [16] gives a detailed description of the CFRP T-beam specimen, so only a brief description is given here. For the experimental T-beam, the density of T700 carbon fibers was $\rho_f = 1.76 g/cm^3$, and the density of matrix was $\rho_m = 1.2 g/cm^3$. The geometry of the 3 Dim and 4 Dir braided composite T-beams, which has been optimized by the simulation discussed below, is shown in Fig. 1. In this study, the T-beam preform was cured into the final composite by TDE86 epoxy resin using a resin transfer molding process. The specimen type, surface braided angle, and $V_f$ of the composite T-beams in the experiments are listed in Table 1.

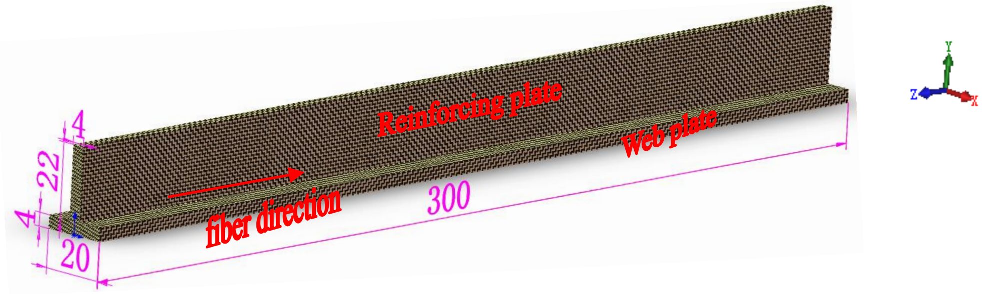

Fig. 1. Geometry of a T-beam specimen (Unit: mm).

Table 1. Structural parameters of the composite T-beam

| Specimen group | specimens | surface braided angle/° | fiber volume fraction* /% |
|---|---|---|---|
| A1 | A1-1 | 20 | 51.3 |
| | A1-2 | 22 | 50.0 |
| | A1-3 | 21 | 51.7 |
| A2 | A2-1 | 29 | 50.1 |
| | A2-2 | 28 | 51.3 |
| | A2-3 | 28 | 51.6 |
| A2 | A3-1 | 35 | 51.4 |
| | A3-2 | 35 | 50.9 |
| | A3-3 | 35 | 50.7 |

*The average of fiber volume fraction within the group is 51.0%; the standard deviation of fiber volume fraction within the group is 0.59 and the dispersion coefficient of fiber volume fraction within the group: 0.01.

### 2.2 Characterization

The influence of different microstructure parameters on the vibration modal properties of the composite T-beam was characterized and the experimental process is shown in Fig. 2. The low end of the T-beam is fixed and the length of the free end of the cantilever to the top is 255 mm. The T-beam was impacted at point B (located on the center line of the web plate along the fiber direction with a distance of 25 mm from the bottom end) by a force transducer (BZ1201) positioned at the hammer, to obtain the excitation signal as a function of time. A miniature pick-up accelerometer (LC0408T) weighing 2.8 g and with sensitivity of 4.4 pc/g was attached at test point A (in the same line as point A with a distance of 25 mm to the top of the T-beam) to receive the response. The input force signal and the output acceleration signals were fed to a dual channel power amplifier (WS2401) and an AD converter (WS5921). Finally, these signals were analyzed by a PC computer using modal software (Vib'SYS modal analysis system) to obtain the modal parameters, namely the frequency response function, natural frequency, and modal shape of the beam.

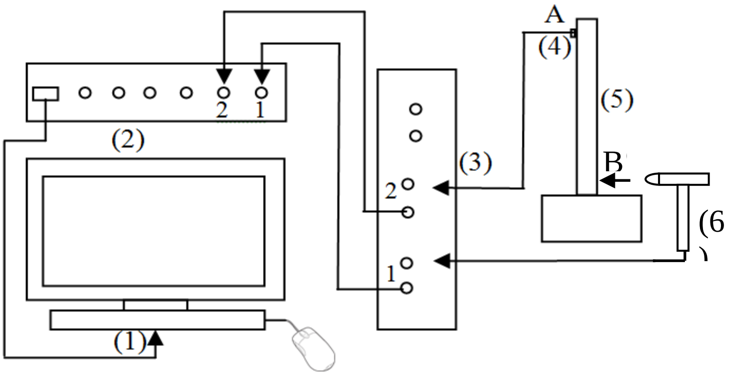

Fig. 2. The vibration modal experiment devices with (1) the modal analysis system Vib′SYS; (2) the net data acquisition instrument WS-5921; (3) the filter amplifier WS-2401; (4) the accelerometer LC0408T; (5) the T beam specimen and (6) the impulse hammer (force transducer BZ1210).

## 3 RESULTS AND DISCUSSION

### 3.1 Effect of surface braided angle on transfer function

To ensure the accuracy of the load on the T-beam, the end of the T-beam must have sufficient stability. The displacement of the T-beam under a load excitation must be sufficiently small and, in the case of initial displacement or acceleration, the structure may effectively reduce the vibration energy and further reduce the load to stabilize the T-beam. The transfer function spectra of the composite T-beam were measured experimentally using the test setups. Under the same impact conditions, lower total vibration energy and higher dissipated structural energy were obtained. With the same impact force, with an increase in the surface braided angle, the amplitude of the T-beam in the first and second order resonance regions was clearly reduced and the corresponding natural frequency was also reduced.

When the natural frequency increased the damping ratio decreased, the damping properties deteriorated, and the ability to transform vibration energy into heat energy decreased. The spectra of the transfer function for the T-beam with the same $V_f$ show that, under transient impact action, the stiffness properties of the T-beam decreased with the increase in the surface braided angle. The braided composite T-beam with a large surface braided angle was more prone to resonance than that with a small surface braided angle. In the design of a T-beam, therefore, it is necessary to develop a full account of the relationship between the stiffness properties and damping performance. Through appropriate design of the structural parameters of the T-beam, the stability of the T-beam structure in the dynamic load condition can be guaranteed, thereby avoiding resonance of the structure when in service in the surrounding environment.

### 3.2 Effect of surface braided angle on damping properties

A small transient impact was applied to the T-beam, which could vibrate freely. Due to the action of structural damping, the vibration decayed gradually. The curves show that the amplitude decayed exponentially with time. The larger the surface braided angle, the faster decay occurred. The time-domain response of the degree of damping oscillation varied with changes in the surface braided angle. Under the same $V_f$, the large surface braided angle in the composite T-beam produced a low oscillation amplitude and a fast speed of amplitude decay. Thus, the greater the surface braided angle of the composite T-beam, the more significant was the damping effect of the impact load. The damping properties of the T-beam, i.e., the logarithmic attenuation ratio $\eta$, damped coefficient $\varepsilon$, and loss factor $\tan\delta$, could be calculated from the time-domain response curves. The results are listed in Table 2. As can be seen from Table 2, when the surface braided angle increased, the logarithmic attenuation ratio and the loss factor increased accordingly.

Table 2. Damping properties of the composite T-beam (average values)

| Specimen group | $\eta$ /% | $\varepsilon$ | $\tan\delta$ /% |
|---|---|---|---|
| A1 | 0.16 | 0.50 | 0.05 |
| A2 | 0.38 | 0.99 | 0.12 |
| A3 | 0.85 | 1.68 | 0.27 |

The dynamic characteristic parameters, namely the damping ratio and the natural frequency of the T-beam, were obtained by experimental modal analysis. The coefficients of variation are shown in Table 3, with the maximum coefficient of variation of damping ratio of 25.10 %. Fig. 3 shows the dependence of the first and second damping ratios of the composite T-beam on the surface braided angle. The first and second damping ratios of the T-beam increased with the increase of the surface braided angle. That is because the macroscopic damping properties of the composite T-beam were mainly affected by the fiber/matrix interface. The damping characteristics were affected by the boundary condition, including ideal bonding or partial bonding. In the ideal situation, the fiber/matrix interface only played the role of transferring loads, which would not have an impact on the damping properties. However, the interface is normally in a non-ideal state. In that case, the mechanical properties and stress state of the interface were closely associated with the composite damping properties. The bond strength of the interface, the angle between the fiber and the load, and the degree of damaged interface all affect the damping properties. When the surface braided angle became large, the fibers had a high bending curve and the porosity of the material and the number of microcracks and other defects would increase, clearly causing a creep effect of the material. Because of these responses, the vibration energy of the composite with a large surface braided angle dissipated more easily. Therefore, when the surface braided angle increased, the damping properties of the T-beam would improve [12].

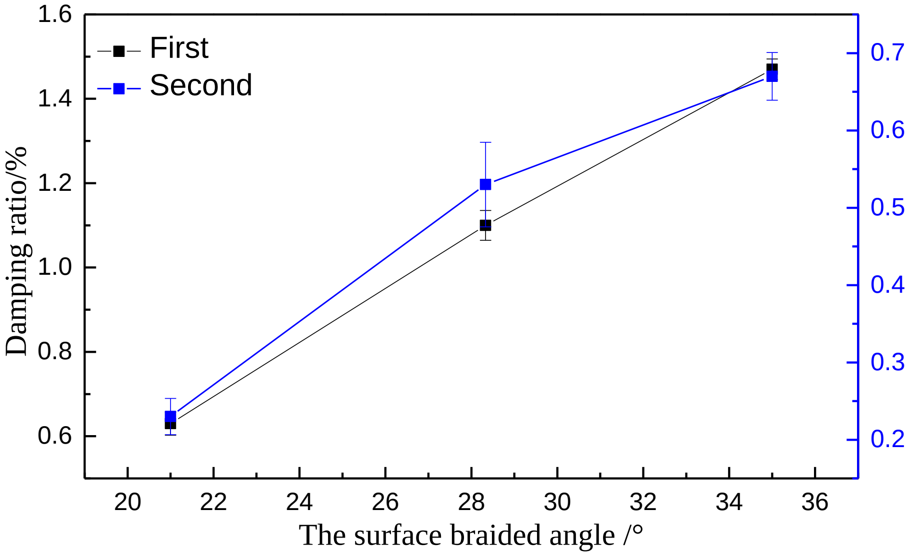

Fig. 3. Damping ratio of the 3 Dim and 4 Dir braided composite T-beam with different surface braided angles.

Table 3 Dynamic parameters of mode experiment samples of the 3D braided composites

| Specimen group | $\xi$ /% | | Coefficient of variation/% | | Frequency | | Coefficient of variation/% | |
|---|---|---|---|---|---|---|---|---|
| | 1st | 2nd | 1st | 2nd | 1st | 2nd | 1st | 2nd |
| A1 | 0.63 | 0.23 | 9.16 | 25.10 | 306.29 | 1858.82 | 1.98 | 0.37 |
| A2 | 1.10 | 0.53 | 9.09 | 10.89 | 261.28 | 1616.06 | 4.09 | 0.05 |
| A3 | 1.47 | 0.67 | 10.39 | 8.62 | 198.74 | 1297.41 | 0.79 | 0.56 |

### 3.3 Effect of surface braided angle on natural frequency

The natural frequency of the T-beam is an important index for measuring the beam's performance. The natural frequency can reflect the stiffness of the structure, and in the design process, the phenomenon of closed frequency should be avoided. The average natural frequency of the composite T-beam and coefficient of variation are listed in Table 3. As is evident, the maximum coefficient of the frequency variation did not exceed 6%; therefore, the natural frequencies obtained from three specimens of the same group had good consistency. This demonstrates that the preformed and the final fabricated braided composites had good uniformity. Fig. 4 shows the different conditions of the natural frequencies varying with the braided angles, indicating that when the $V_f$ was held constant, the first and the second natural frequencies decreased with the increase of the braided angle.

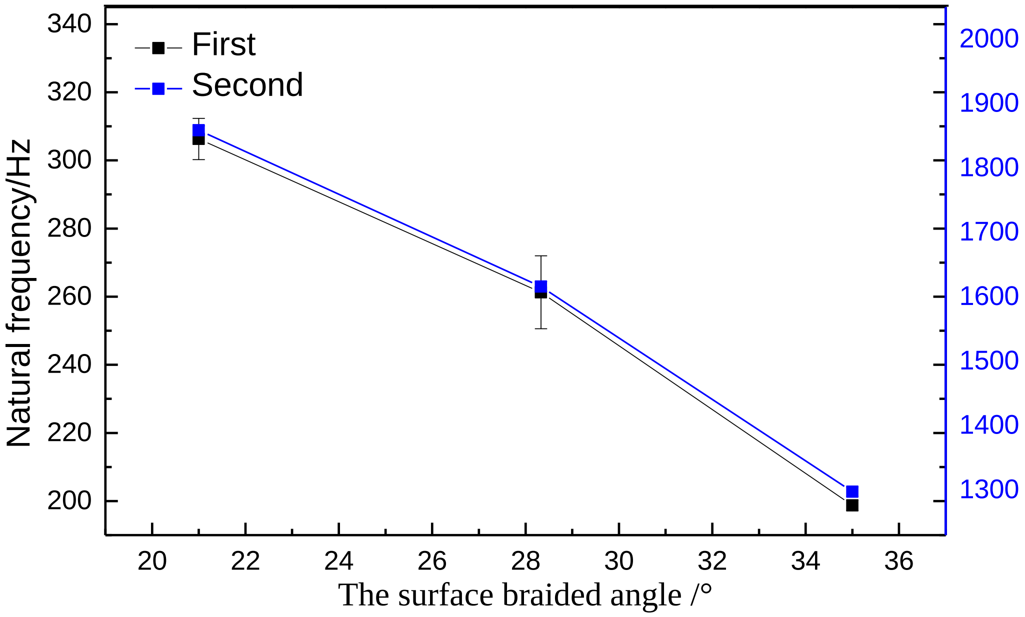

Fig. 4. Natural frequency of the 3 Dim and 4 Dir braided composite T-beam with different surface braided angles.

In the cantilever boundary conditions, when the composite T-beam vibrated, its natural frequency was proportional to the square root of the elastic modulus. When the $V_f$ was held constant, a larger braided angle resulted in a lower elastic modulus of the material. Therefore, the natural frequency of material with a large braided angle was lower than that with a small braided angle. As the natural frequency is determined by the mass, stiffness, shape, and boundary conditions of the structure, a reasonable choice of braided angle has a significant effect on the natural frequencies of the T-beam. Comparison and analysis of the results of the vibration modal parameters of the composite T-beams with different structural parameters indicated that the Young's modulus and material density had dramatic effects on the vibration modal parameters. As the density difference between the carbon fiber and epoxy resin was small, the density effect could be ignored. Therefore, the dominating factor affecting vibration modal parameters was the Young's modulus. The fiber bundle and the braided axial formed a certain angle (γ), that is, a braided angle within the composite T-beam [29, 34]. When the $V_f$ was held constant in the composite, the fiber bundle was extended in a straight line. When the fiber bundle meets the boundary of the composite material, it was in a state of refraction. The same fiber bundle in the composites was in the spatial orientation, not in the plane orientation. The trend of the interior braided yarns was to become straighter with a decrease of the braided angle. Thus, the axial strength and elastic modulus of the T-beam and the natural frequencies increased.

Fig. 5 summarizes the results obtained from the vibration modal experiments for all the composite T-beams, representing the loss factor as a function of the natural frequency. The frequency map determined the first frequency in a range from 196 to 341 Hz and the second frequency in a range from 1288 to 1865 Hz. The A3 composite T-beam resulted in the best damping properties under defined frequencies. The frequency of A1 composite T-beam was the highest, but its damping property was poor. The relationship of loss factor and natural frequency provided a selection basis for designing the composite T-beam.

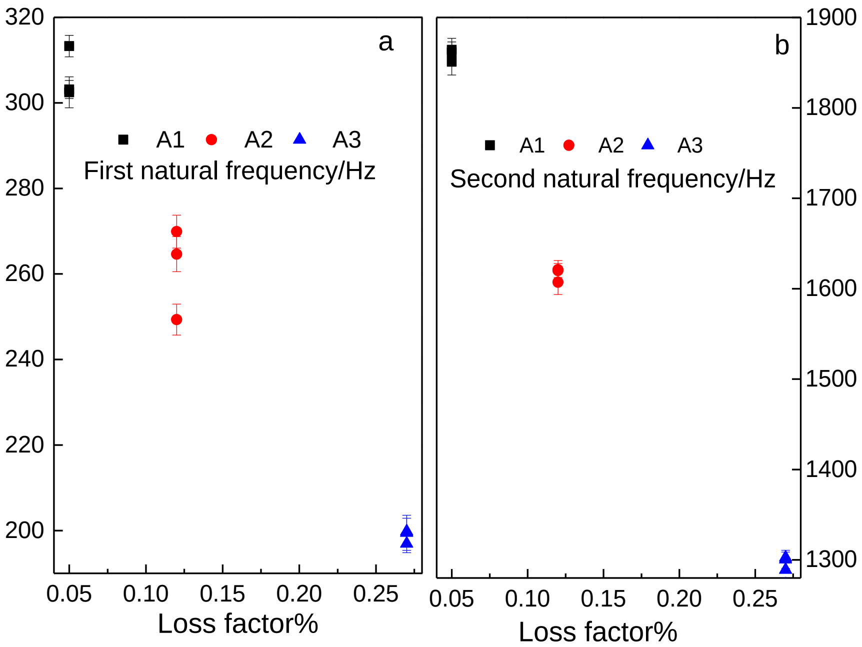

Fig. 5. Loss factor determined by a vibration beam experiment as a function of the (a) first and (b) second natural frequency.

### 3.4 Modal shapes of the composite T-beam

When a structure vibrates at a frequency close to one of its natural frequencies, the mode shape is the relative ratio of displacement between each point in the structure. The mode shape relates to the physical characteristics e.g., mass, stiffness of the vibration system, and boundary conditions, but has nothing to do with the excitation of an external input [13]. In practical application, this feature can be used to determine the location of damage . In the modal vibration test, we first had to deal with the data relating to the real and imaginary parts of the frequency response function, and then the modal shapes of the T-beam were obtained from the amplitude and direction of the imaginary part of the natural frequency. The modal shapes corresponding to the two frequencies of the T-beam are shown in Fig. 6. There being little change in the structure, there was no difference in the modal shapes. Thus, the modal shapes obtained in the vibration modal experiments did not reflect the differences in the braided angle in the composite T-beam, i.e., differences in the braided angle had no obvious effect on the modal shapes [14].

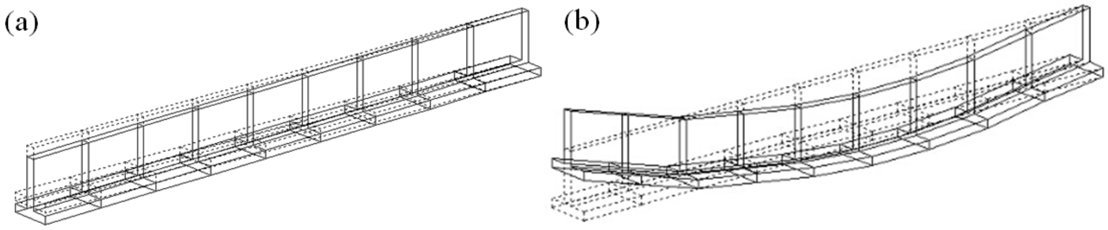

Fig. 6. Experimental modal shapes of a T-beam (a) the first modal shape and (b) the second modal. shape.

## 4 FINITE ELEMENT ANALYSIS

The natural frequencies and modal shapes of a beam were analyzed by FEM. According to the theory of composite material, the 3 Dim and 4 Dir braided composite was a transversely isotropic material, so the selected material properties were orthotropic in the simulation. A SOLID187 element was used to construct the structure. The element was defined by an 8-node element with three degrees of freedom along the x, y, and z directions. The model was divided into the hexahedral meshes. The

Block Lanczos method was used to conduct modal analysis for the T-beam in the boundary conditions of the cantilever and to calculate the natural frequency and modal shape.

### 4.1 Effect of micro structure on natural frequency

The unit cell model of the 3 Dim and 4 Dir T-beam is shown in Fig. 7. In the experiment, measurement of the torsion modal shapes requires at least two sensors placed symmetrically in the reinforcing plate and simultaneously in the web plate. To reduce the impact of the additional mass of the sensor on the modal parameters of the T-beam, only one accelerometer was fixed in the reinforcing plate at the response point during the test to measure. the bending modal shapes. In the FEM calculations, bending modal and torsion modal can be obtained.

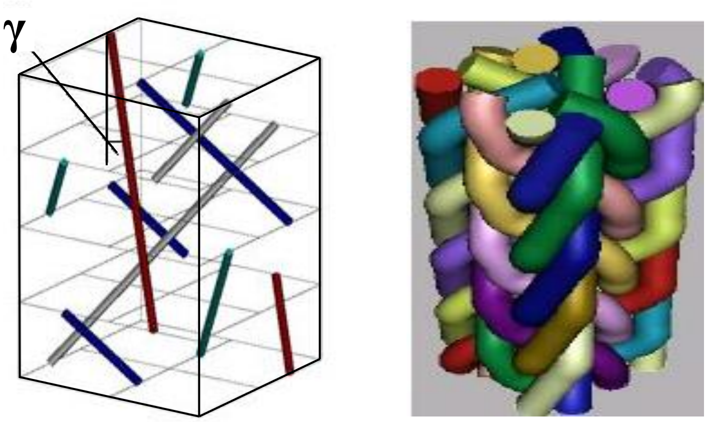

Fig. 7. Unit cell model of the 3 Dim and 4 Dir T-beam (a) interior yarn structure of preformed cell and (b) the unit cell model [13, 15].

The natural frequencies of the T beams with different braided angle obtained by FEM and experiment are listed in Table 4. It can be seen that the natural frequency derived by experiment and simulation matched well, with the minimum error of 5.6% and the maximum error of 9.5%, which was due to the damping factor. The damping term in most vibration modal analysis is not taken into consideration, although damping does have a significant effect on the response amplitude in a dynamic service condition. The reason for this neglect is that for a weak damping system, the natural frequencies and mode shapes that are the most important tasks for vibration modal analysis are almost the same as those for an identical system with damping ignored. Since the damping of CFRP composites is weak and the damping information regarding the 3Dim and 4Dir braided composite was very limited, the damping of the T-beam was not considered in FEM.

Table 4: Natural frequencies of the T beam obtained by the finite element method and by experiment

| Specimen group | Experiment | | | | FEM | |
|---|---|---|---|---|---|---|
| | Mean | | SD/% | | | |
| | 1st | 2nd | 1st | 2nd | 1st | 2nd |
| A1 | 306.29 | 1858.82 | 6.06 | 6.89 | 330.79 | 1966.55 |
| A2 | 261.28 | 1616.06 | 10.69 | 7.73 | 286.15 | 1730.79 |
| A3 | 198.74 | 1297.41 | 1.56 | 7.31 | 211.26 | 1388.22 |

### 4.2 Effect of free end length on natural frequency

The influence of the free end length on the natural frequency of the T beam was simulated by FEM. and shown in Figure 8. As can be seen from Fig. 8, the simulation results of the natural frequency of the T beam were consistent with the experimental results with the smallest percentage difference of 0.7% and the maximum percentage difference of 6.8%. For the same boundary conditions, the same material beams, the natural frequency decreases with the increase of the free end length. This is because the first natural frequency of the beam to the theoretical value were given by Euler–Bernoulli beam theory.

$$\omega_1 = \frac{1.875^2}{2\pi l^2}\sqrt{\frac{(EI)_c}{\rho A}} \tag{1}$$

where ω1 is first natural frequency (Hz), E is storage modulus of the composite beam, l is beam length, ρ is the mass density of the beam, A is the cross-sectional area of the beam, and I is the cross-sectional moment of inertia of the beam about the axis of bending.

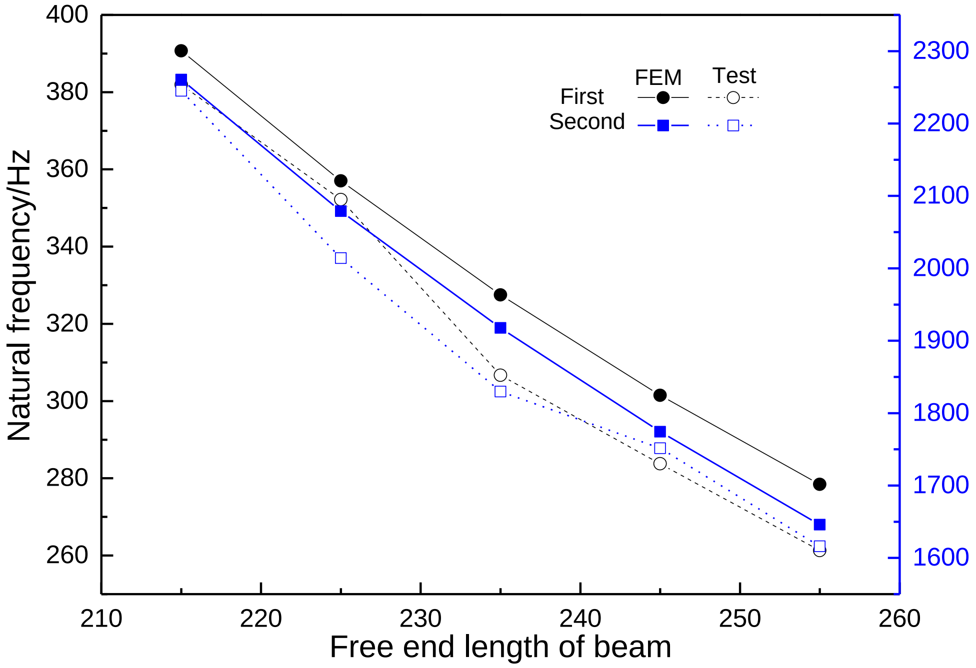

Fig. 8. Natural frequency of the composites as a function of the beam free length.

### 4.3 Effect of reinforcing plate size on natural frequency

In the simulation, the thickness of reinforcing plate and web plate are 3 mm, 4 mm and 5 mm and the width of the web place is always 20 mm. The influence of reinforcing plate width on the natural frequency were studied. The width were 4 mm, 8 mm, 12 mm, 16 mm, 20 mm and 24 mm, respectively. The influence of reinforcing plate width on the natural frequencies is shown in Fig. 9. As can be seen from Fig. 9, the first two order natural frequency of the T beam increased with the increase of reinforcing plate width. In addition, when the reinforcing plate width was fixed, with the increasing of thickness of reinforcing plate and web plate, the natural frequency of T beam increased.

The effects of thickness of reinforcing plate on natural frequency of the T beam were studied. The web size (length × width × thickness) is 255 mm × 20 mm × 4 mm and the size of reinforcing plate is 255 mm × 20 mm (length × width) with the thickness of the reinforcing plate of 2 mm, 4 mm, 6 mm, 8 mm, 10 mm and 12 mm, respectively. The relationship between the thickness of reinforcing plate and the natural frequency was shown in Fig. 10. As can be seen from Fig. 10, the first two order natural frequency of the T beam increased sharply with the increase of the thickness. When the thickness of the reinforcing plate reached a certain value, the frequency decreased slowly with the increase of the thickness. The optimized thickness of the reinforcing plate was 6 mm. When the thickness was less than 6 mm, the change rate of natural frequency was greater than that when the thickness was greater than 6 mm.

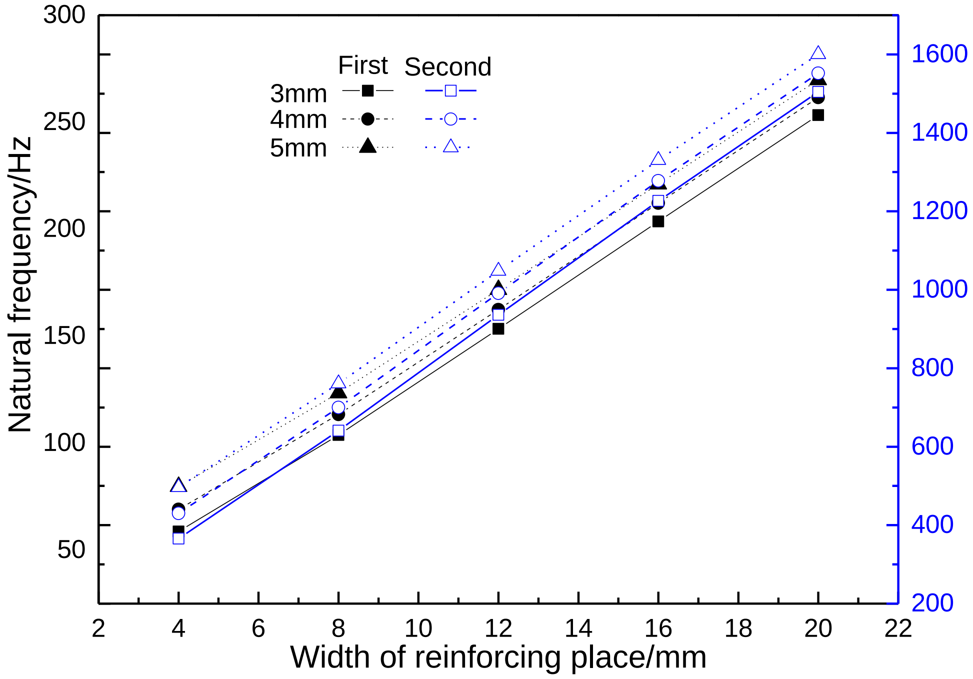

Fig. 9. Natural frequency of the composites as a function of the width of the reinforcing plate.

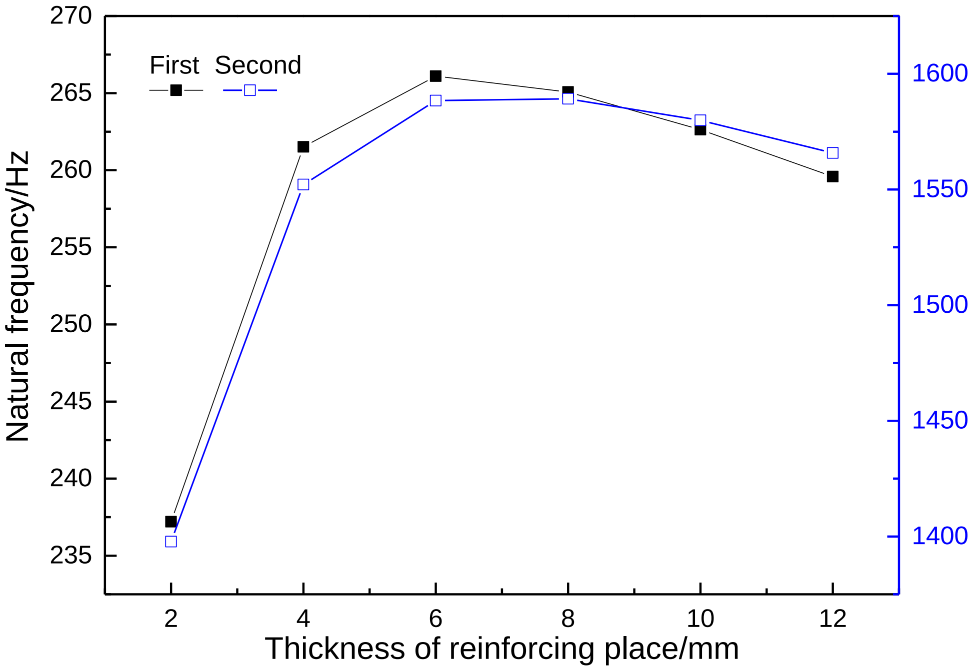

Fig. 10. Natural frequency of the composites as a function of the thickness of the reinforcing plate.

## 5 CONCLUSIONS

Using braided composite T-beams has the advantage of improving the safety performance of a structure, reducing structural weight, decreasing the number of connections and fittings, and lowering manufacturing cost. In this study, the vibration modal properties of 3Dim and 4Dir braided composite T-beams were investigated experimentally and numerically. The relationship between the vibration properties and microstructural parameters was studied. Our analysis has provided a theoretical basis for designing braided composite T-beams and predicting their vibration properties When the $V_f$ was held constant, with a decrease in the braid angle, the natural frequency increased and the damping ratio decreased. Finally, the model of the T-beam was analyzed by finite element simulation. In the boundary conditions of a cantilever, the mode shapes of the T-beam obtained in simulation were identical to those obtained in experiment.

## ACKNOWLEDGEMENTS

The author would like to thank the funding support from the China Postdoctoral Science Foundation funded project (grant number: 2016M591391).

## REFERENCES

1. L. Jiang, G. Xu, S. Cheng, X. Lu and T. Zeng, Predicting the thermal conductivity and temperature distribution in 3D braided composites, *Compos Struct*, **108**, 2014, pp. 578-583.
2. W. Zhang, Z. Pan, R. Gideon, B. Gu and B. Sun, Effects of temperature and strain rate on impact compression behaviors of three-dimensional carbon fiber/epoxy braided composites, *J Compos Mater*, **49**, 2014, pp. 771-782.
3. N. Wu, Y. Liang, K. Zhang, W. Xu and L. Chen, Preparation and bending properties of three dimensional braided single poly (lactic acid) composite, *Compos Part B-Eng*, **52**, 2013, pp. 106-113.
4. D. Li, C. Zhao, T. Ge, L. Jiang, C. Huang and N. Jiang, Experimental investigation on the compression properties and failure mechanism of 3D braided composites at room and liquid nitrogen temperature, *Compos Part B-Eng*, **56**, 2014, pp. 647-659.
5. T. P. Vo, J. Lee, K. Lee and N Ahn, Vibration analysis of thin-walled composite beams with I-shaped cross-sections, *Compos Struct*, **93**, 2011, pp. 812-820.
6. F. Minghini, N. Tullini and F. Laudiero, Vibration analysis with second-order effects of pultruded FRP frames using locking-free elements, *Thin-wall Struct*, **47**, 2009, pp. 136-150.
7. V. X., Tran, S. Geniaut, E. Galenne and I. Nistor, A modal analysis for computation of stress intensity factors under dynamic loading conditions at low frequency using extended finite element method, *Eng Fract Mech*, **98**, 2013, pp. 122-136.
8. I. Yesilyurt and H. Gursoy, Estimation of elastic and modal parameters in composites using vibration analysis, *J Vib Control*, **21**, 2015, pp. 509-524.
9. C. Kyriazoglou and F. J. Guild, Finite element prediction of damping of composite GFRP and CFRP laminates-a hybrid formulation-vibration damping experiments and Rayleigh damping, *Compos Sci Technol*, **66**, 2006, pp. 487-498.
10. G. Jin, C. Yang, Z. Liu, S. Gao and C Zhang, A unified method for the vibration and damping analysis of constrained layer damping cylindrical shells with arbitrary boundary conditions, *Compos Struct*, **130**, 2015, pp. 124-142.
11. D. Li, Z. Lu and J. Li, Experimental research on the vibration damping properties of 3D braided composites, *J Mech Strength*, **31**, 2009, pp. 211-214.
12. Y. Gao, and J. Li, Effects of braiding angle on modal experimental analysis of three-dimensional and five-directional braided composites, *Compos Part B-Eng*, **43**, 2012, pp. 2423-2428.
13. X. Pei, J. Li, K. Chen and G Ding, Vibration modal analysis of three-dimensional and four directional braided composites, *Compos Part B-Eng*, **69**, 2015, pp. 212-221.
14. L. Chen, X. M. Tao and C. L. Choy, Mechanical analysis of 3-D braided composite by the finite multiphase element method, *Compos Sci Technol*, **59**, 1999, pp. 2383-2391.
15. J. Li and Q. Liu, A study on fibre tows' orientation for 3-D braided composites, *J Text Res*, **20**, 1999, pp. 203-206.
16. X. Pei, L. Chen, J. Li, Y. Tang and K. Chen, Effect of damage on the vibration modal of a novel three-dimensional and four-directional braided, *Compos Part B-Eng*, **86**, 2016, pp.108-119.